

A New Quaternary Nitride, $\text{Li}_3\text{Ba}_2\text{NbN}_4$

X. Z. Chen and H. A. Eick¹

Department of Chemistry and Center for Fundamental Materials Research, Michigan State University, East Lansing, Michigan 48824-1324

Received January 28, 1994; in revised form April 5, 1994; Accepted April 7, 1994

A new quaternary nitride, $\text{Li}_3\text{Ba}_2\text{NbN}_4$, has been synthesized from Li, Ba, and Nb metals under flowing N_2 at 850°C. The structure, as determined by single-crystal X-ray diffraction, is monoclinic, space group $C2/c$ with $Z = 4$, and has lattice parameters $a = 11.296(2)$ Å, $b = 5.673(1)$ Å, $c = 11.347(2)$ Å, and $\beta = 121.456(8)^\circ$. Refinement based upon F^2 yielded $R2 = 0.073$ and $wR2 = 0.105$. (For comparison, a refinement based upon F yielded $R1 = 0.043$). The Nb and one of the two independent Li ions are coordinated tetrahedrally by N anions; the Li tetrahedra are distorted. By sharing edges, the Nb and Li tetrahedra form chains which are linked by the remaining Li ions to form the three-dimensional structure. The Ba ions are located between the Li-Nb chains. © 1994 Academic Press, Inc.

INTRODUCTION

There has recently been a resurgence of interest in transition metal nitrides as materials with potentially interesting magnetic and electronic properties (1). Some recently reported structures of transition metal-containing ternary nitrides include Ca_3CrN_3 (2), Ca_3VN_3 (3), M_3FeN_3 (4), and M_3MnN_3 ($M = \text{Ba}, \text{Sr}$) (5). All have trigonal planar $[\text{M}^{\text{III}}\text{N}_3]^{6-}$ anions with either C_{2v} ($M^{\text{III}} = \text{V}$ and Cr) or D_{3h} ($M^{\text{III}} = \text{Fe}$ and Mn) symmetries. Other recent examples include $\text{Fe}_3\text{Mo}_3\text{N}$ (6), FeWN_2 (7), Ba_3MN_4 ($M = \text{Mo}, \text{W}$) (8), Ca_2ZnN_2 (9), and LiMoN_2 (10), a metallic, layered ternary nitride from which the Li atoms can be deintercalated and reintercalated.

Other long-known examples of ternary nitride compounds include antiperovskite-type MT_3N compounds (11) such as ZnMn_3N , anti-fluorite-type Li_7MN_4 ($M = \text{V}, \text{Mn}$) and Li_9CrN_4 (12), and anti- La_2O_3 -type Li_2ZrN_2 and Li_2CeN_2 (13).

Very few Nb-containing ternary nitrides have been reported and no quaternary nitride appears to have been synthesized. With the exception of $\text{LiBa}_4\text{M}_2\text{N}_7$ ($M = \text{W}, \text{Mo}$) (14), which contains dimeric tetrahedral anions, most quaternary transition metal-containing nitrides involve Li-M-Ni-N systems, where $M = \text{Ca}, \text{Sr},$ or Ba (15). In $\text{LiSr}_2\text{CoN}_2$ (16) and $\text{M}_2\text{LiFe}_2\text{N}_3$ ($M = \text{Ba}$ or Sr)

(17), the $[\text{Co}^{\text{I}}\text{N}_2]^{5-}$ and $[\text{Fe}_2\text{N}_3]^{5-}$ anions, respectively, were characterized.

Recently we reported the synthesis and structure of $\text{Li}_3\text{Ba}_2\text{Ta}_2\text{N}_4$ (18), in which the Ta and one of the two independent Li atoms are tetrahedrally coordinated by N atoms. Since Ta^{V} and Nb^{V} have almost identical ionic radii and form some isostructural nitrogen-containing compounds, e.g., Li_7NbN_4 (19) and $\text{Li}_7\text{Ta}_2\text{N}_4$ (20), $\text{Ba}_2\text{Ta}_2\text{N}_3$ (21), and $\text{Ba}_2\text{Nb}_2\text{N}_3$ (22), we expected the related Nb compound to be preparable. We report the synthesis and structure of the quaternary nitride, $\text{Li}_3\text{Ba}_2\text{NbN}_4$.

EXPERIMENTAL

Synthesis. A mixture of elemental Li, Ba (99.7%, Cerac, Inc.), and Nb powder (99%, E. H. Sargent & Co., 80 mesh) in a 2:1:1 molar ratio was confined in a Nb boat which was then placed in a quartz reaction tube. The mixture was first heated under flowing Ar (AGA Gas, Inc.) to 850°C at a rate of 97°C/hr, held at this temperature under flowing nitrogen (AGA Gas, Inc.) for 24 hr, and then cooled to 150°C under Ar at a rate of 10.8°C/hr. Pale yellow single crystals of $\text{Li}_3\text{Ba}_2\text{NbN}_4$ were isolated from the crushed product which was both air and moisture sensitive. Both the Ar and N_2 gases were purified by molecular sieves (4-8 mesh, Aldrich) and De-Ox catalyst (Johnson Matthey). Typical moisture and oxygen contents of the gases were <0.5 and <1 ppm, respectively.

Structure determination. An irregular crystal of approximate dimensions 0.120 × 0.080 × 0.080 mm was selected and sealed in a 0.1-mm glass capillary in a N_2 -filled glove bag. All measurements were made on a Rigaku AFC6S 4-circle diffractometer with graphite-monochromated $\text{MoK}\alpha$ radiation ($\lambda = 0.71069$ Å). Lattice parameters were obtained by least-squares refinement of the angle settings of 23 carefully centered reflections in the range $22.26^\circ < 2\theta < 29.00^\circ$. The choice of space groups was reduced to $C2/c$ and Cc by systematic absences ($h0l, l \neq 2n$; $hkl, h + k \neq 2n$), and the structure were solved based on space group $C2/c$ (No. 15). The lattice parameters and color also suggested an

¹ To whom correspondence should be addressed.

TABLE 1
Summary of Crystal and Diffraction Data for Li₃Ba₂NbN₄

| | |
|---|--|
| Chemical formula | Li ₃ Ba ₂ NbN ₄ |
| Formula weight | 444.42 |
| Space group | C2/c |
| <i>a</i> , <i>b</i> , <i>c</i> (Å) | 11.296(2), 5.673(1), 11.347(2) |
| β (°) | 121.456(8) |
| <i>V</i> (Å ³) | 620.3(2) |
| <i>Z</i> | 4 |
| <i>D</i> _{calc} (g/cm ³) | 4.759 |
| <i>T</i> (°C) | 23 ± 1 |
| Crystal color, Habit | Pale yellow, irregular |
| Crystal dimensions (mm) | 0.120 × 0.080 × 0.080 |
| 2θ max (°) | 65.0 |
| Scan type | ω-2θ |
| X-ray radiation (λ) | MoKα (λ = 0.71069 Å) |
| Monochromator | Graphite |
| Octants collected | <i>hkl</i> ; <i>hk-l</i> |
| Absorption coeff μ (cm ⁻¹) | 142.0 |
| Measured reflections | 1079 |
| Observed reflections ^a | 764 |
| Unique reflections | 1038 |
| F000 | 760 |
| Number of variables | 48 |
| Max (min) peak in final diff. map | 4.25 (-3.07) e/Å ³ |
| <i>R</i> ² , <i>wR</i> ² ^c | 0.073, 0.105 |

^a *I* > 3.00σ(*I*)

^b *R*² = Σ|*F*_o² - *F*_c²|/Σ*F*_o²

^c *wR*² = [Σ*w*(|*F*_o² - *F*_c²)²]/Σ(*wF*_o²)²]^{1/2}

isostructural relationship with Li₃Ba₂TaN₄. The integral relationship between the *b* and *c* lattice parameters was of particular concern, but cell reduction programs did not identify a reasonable higher symmetry cell.

Data were collected at 23 ± 1°C by the ω-2θ scan technique to 2θ ≤ 65°. Of the 1079 reflections which were collected, 1038 were unique. The intensities of 3 repre-

sentative reflections which were measured after every 150 reflections declined by 0.45%. A linear correction factor was applied to account for this phenomenon. The linear absorption coefficient for MoKα radiation, 142.0 cm⁻¹, was used to make an empirical absorption correction which resulted in transmission factors that ranged from 0.81 to 1.00. The data were corrected for Lorentz and polarization effects and for secondary extinction (coefficient = 0.27 ± 0.05 × 10⁻⁶).

The structure was solved by direct methods with the program SHELXS86 (23). All atoms were refined anisotropically with the refinement based upon *F*². The final cycle of full-matrix least-squares refinement (24), which was based on 764 observed reflections (*I* > 3.00σ(*I*)) and 48 variable parameters, converged with unweighted and weighted agreement factors of

$$R2 = \frac{\sum |F_o^2 - F_c^2|}{\sum F_o^2} = 0.073$$

$$wR2 = \frac{[\sum w(|F_o^2 - F_c^2|)^2 / \sum (wF_o^2)^2]^{1/2}}{1} = 0.105.$$

For comparison, a refinement of the overall scale factor on *F* with the final parameters and 764 observed reflections (*I* > 3σ(*I*)) led to

$$R1 = \frac{\sum ||F_o| - |F_c||}{\sum |F_o|} = 0.043.$$

The maximum and minimum peaks in the final difference Fourier map, 4.25 and -3.07 e/Å³, respectively, are close to either Ba or Nb atoms.

Neutral atom scattering factors were taken from Cromer and Waber (25). All calculations were performed with the TEXSAN (26) crystallographic software package. Data collection and atomic position parameters are listed in Tables 1 and 2, respectively. Thermal parameters (*U*_{ij}) are presented in Table 3.

TABLE 2
Atomic Positions and *B*(eq) for Li₃Ba₂NbN₄

| Atom | <i>x</i> | <i>y</i> | <i>z</i> | <i>B</i> (eq) (Å ²) |
|-------|------------|------------|------------|---------------------------------|
| Nb | 0 | 0.1118(3) | 0.25 | 0.49(4) |
| Ba | 0.20933(7) | -0.0359(1) | 0.11209(7) | 0.84(3) |
| N(1) | 0.164(1) | -0.088(2) | 0.337(1) | 0.8(3) |
| N(2) | 0.001(1) | 0.318(2) | 0.113(1) | 1.2(3) |
| Li(1) | 0 | -0.365(6) | 0.25 | 3(1) |
| Li(2) | 0.384(2) | -0.052(5) | 0.458(2) | 1.6(8) |

Note. The equivalent isotropic temperature factor is defined as (28)

$$B(\text{eq}) = \frac{8\pi^2}{3} \left[\sum_{i=1}^3 \sum_{j=1}^3 U_{i,j} a_i^* a_j^* \mathbf{a}_i \cdot \mathbf{a}_j \right]$$

TABLE 3
Anisotropic Thermal Parameters, U_{ij} , for $\text{Li}_3\text{Ba}_2\text{NbN}_4$

| Atom | U_{11} | U_{22} | U_{33} | U_{12} | U_{13} | U_{23} |
|-------|-----------|-----------|-----------|-----------|-----------|-----------|
| Nb | 0.0062(6) | 0.0046(6) | 0.0071(6) | 0 | 0.0030(5) | 0 |
| Ba | 0.0091(3) | 0.0110(4) | 0.0108(4) | 0.0002(2) | 0.0045(2) | 0.0010(2) |
| N(1) | 0.006(4) | 0.014(5) | 0.011(4) | 0.006(3) | 0.003(3) | 0.003(3) |
| N(2) | 0.016(5) | 0.015(5) | 0.015(5) | -0.002(4) | 0.009(4) | 0.003(4) |
| Li(1) | 0.01(2) | 0.01(2) | 0.07(3) | 0 | 0.01(2) | 0 |
| Li(2) | 0.01(1) | 0.03(1) | 0.02(1) | 0.010(9) | 0.002(8) | 0.01(1) |

Note. The anisotropic temperature factor coefficients U_{ij} are defined as

$$\exp(-2\pi^2(a^*U_{11}h^2 + b^*U_{22}k^2 + c^*U_{33}l^2 + 2a^*b^*U_{12}hk + 2a^*c^*U_{13}hl + 2b^*c^*U_{23}kl)).$$

RESULTS AND DISCUSSION

The crystal structure of $\text{Li}_3\text{Ba}_2\text{NbN}_4$ is identical to that of $\text{Li}_3\text{Ba}_2\text{Ta}_2\text{N}_4$ (18). Selected bond distances and angles are given in Table 4. The Nb and Li(1) atoms are coordinated tetrahedrally by two N(1) and two N(2) atoms (Fig.

1), with the Li tetrahedra distorted as bond lengths indicate. These Nb and Li tetrahedra share edges to form along b parallel chains which are then linked together by Li(2) atoms to form the three-dimensional network. The M -N(1) and M -N(2) bond lengths in $\text{Li}_3\text{Ba}_2\text{MN}_4$, $M = \text{Nb}$, are 1.948(9) and 1.95(1) Å, and, $M = \text{Ta}$, 1.962(6) and

TABLE 4
Selected Bond Distances (Å) and Angles (°) in $\text{Li}_3\text{Ba}_2\text{NbN}_4$

| Bond distances | | Bond angles | |
|----------------|-------------|--------------------|------------|
| Nb-N(1) | 1.948(9) | N(1)-Nb-N(1) | 108.9(6) |
| Nb-N(2) | 1.95(1) | N(1)-Nb-N(2) | { 110.7(4) |
| Li(1)-N(1) | 2.23(3) | | { 110.1(4) |
| Li(1)-N(2) | 2.38(3) | N(2)-Nb-N(2) | 106.3(7) |
| Li(2)-N(1) | 2.12(2) | N(1)-Li(1)-N(1) | 90(1) |
| Li(2)-N(2) | { 1.99(2) | Li(1)-Nb-Li(1) | 180.00(0) |
| | { 2.05(2) | Nb-Li(1)-Nb | 180.00(0) |
| Ba-N(1) | { 2.87(1) | N(1)-Li(2)-N(2) | 129(1) |
| | { 2.97(1) | | 119(1) |
| | { 2.82(1) | N(2)-Li(2)-N(2) | 109(1) |
| Ba-N(2) | { 3.10(1) | N(2)-Li(1)-N(2) | 82(1) |
| | { 2.90(1) | Nb-N(1)-Li(1) | 80.3(7) |
| | { 3.23(1) | Nb-N(2)-Li(1) | 85.9(7) |
| Nb-Li(1) | { 2.70(4) | Li(1)-N(2)-Li(2) | { 102(1) |
| | { 2.97(4) | | { 81(1) |
| Nb-Ba | { 3.5503(9) | Li(2)-N(2)-Li(2) | 71(1) |
| | { 3.5381(1) | Nb-N(1)-Li(2) | 133.9(5) |
| | { 3.444(1) | Li(1)-N(1)-Li(2) | 145.2(8) |
| Li(1)-Ba | { 2.97(1) | Nb-N(2)-Li(2) 2× | 144.3(9) |
| | { 3.92(2) | N(1)-Li(1)-N(2) 2× | 122.1(4) |
| Li(2)-Ba | { 3.35(2) | | |
| | { 2.90(3) | | |
| | { 3.29(2) | | |
| | { 3.07(2) | | |
| Li(1)-Li(2) | { 2.90(2) | | |
| | { 3.41(3) | | |
| Li(2)-Li(2) | 2.35(4) | | |
| Ba-Ba | { 4.056(2) | | |
| | { 3.960(1) | | |
| | { 3.956(2) | | |

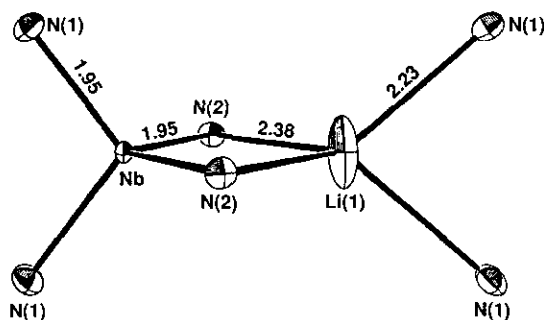


FIG. 1. Edge-shared Nb and Li(1) tetrahedra. Note how the distortion in the Li tetrahedra contrasts with the regularity of the Nb tetrahedra. Distances are in Å.

1.942(7) Å (18), respectively, consistent with those in Li_7NbN_4 (1.95 Å) (19), where Nb atoms are comparably coordinated by N atoms. Most bond distances in $\text{Li}_3\text{Ba}_2\text{NbN}_4$ are identical within error limits to those in $\text{Li}_3\text{Ba}_2\text{Ta}_2\text{N}_4$ (18).

The environments of the two kinds of Li atoms differ. A layered fragment devoid of Ba atoms that shows the Li(2)–N(1) bond which is perpendicular to the bc plane can be viewed in the bc plane as shown in Fig. 2. The Li(2) atoms are in the center of a slightly distorted trigonal plane comprised of one N(1) atom and two N(2) atoms such that each Li(2) atom links three Li(1)–Nb chains.

The edge-sharing of the $[\text{NbN}_4]$ and $[\text{LiN}_4]$ tetrahedra is similar to that observed in the molecular tetrathimetalates, $\text{Li}_3[\text{MS}_4] \cdot 2 \text{TMEDA}$ ($M = \text{V}, \text{Nb}, \text{Ta}$; TMEDA = N, N, N', N' -tetramethylethylenediamine) (27), where $[\text{MS}_4]^{3-}$ ion interact with Li atoms by edge sharing to form a linear chain. In $\text{Li}_3\text{Ba}_2\text{NbN}_4$ the bond angles N(2)–

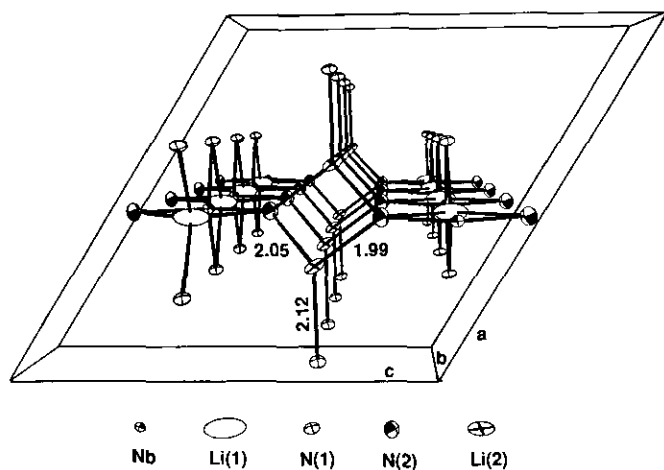


FIG. 2. The layered structure of the Li(2) atoms bridges the Li(1)–Nb chains. The three-dimensional network is cut above and below the Li(2)–N(1) bonds. Ba atoms are omitted for clarity.

Nb–N(2) (106.3°) and N(1)–Nb–N(1) (108.9°) are smaller than the N(1)–Nb–N(2) angles (avg. 110.4°), suggestive that the smaller angles result because of the Li(1)–N interactions. The interactions of the three-coordinated Li(2) atoms (which have short Li(2)–N(1) and Li(2)–N(2) distances) with the N(1) atoms probably causes the N(1)–Nb–N(1) angle to be larger than the N(2)–Nb–N(2) angle. The bond angle variations N(2)–Li(1)–N(2) (82°) < N(1)–Li(1)–N(1) (90°) < N(1)–Li(1)–N(2) (avg. 122.2°) can be explained in the same way. Comparable angular relationships were observed in the tetrathimetalates. The major difference between this nitride structure and those of the tetrathimetalates is that in the latter the linear chains are not linked together by Li(2) atoms. Instead, the chains are connected to the TMEDAs through Li(2) atoms which are located in tetrahedral sites formed by two sulfur and two nitrogen atoms.

The Ba atoms in $\text{Li}_3\text{Ba}_2\text{NbN}_4$ are located between the Li(1)–Nb chains and serve to balance charges. Each Ba^{II} ion has four nearest N(1) and four nearest N(2) neighbors whose distances range from 2.82 to 3.39 Å. Comparable values in $\text{Ba}_2\text{Ta}_2\text{N}_3$ (21) range from 2.771 to 3.462 Å and in Ba_3MoN_4 (8) from 2.654 to 3.566 Å. Two sets of two N(1) and two N(2) atoms describe trapezoids that comprise the arcs of a distorted dodecahedron (18).

ACKNOWLEDGMENTS

We thank Dr. D. L. Ward and Dr. X. Zhang for helpful suggestions regarding data collection and structure solution procedures.

REFERENCES

1. F. J. DiSalvo, *Science* **247**, 649–655 (1990).
2. D. A. Vennos, M. E. Badding, and F. J. DiSalvo, *Inorg. Chem.* **29**, 4059–4062 (1990).
3. D. A. Vennos and F. J. DiSalvo, *J. Solid State Chem.* **98**, 318–322 (1992).
4. P. Höhn, R. Kniep, and A. Rabenau, *Z. Kristallogr.* **196**, 153–158 (1991).
5. A. Tennstedt, C. Röhr, and R. Kniep, *Z. Naturforsch. B.* **48**, 794–796 (1993).
6. D. S. Bem, C. P. Gibson, and H.-C. zur Loye, *Chem. Mater.* **5**, 397–398 (1993).
7. D. S. Bem and H.-C. zur Loye, *J. Solid State Chem.* **104**, 467–469 (1993).
8. A. Gudat, P. Höhn, R. Kniep, and A. Rabenau, *Z. Naturforsch. B.* **46**, 566–572 (1991).
9. M. Y. Chern and F. J. DiSalvo, *J. Solid State Chem.* **88**, 528–533 (1990).
10. S. H. Elder, L. H. Doerrer, and F. J. DiSalvo, *Chem. Mater.* **4**, 928–937 (1992).
11. R. Fruchart, R. Madar, M. Barberon, E. Fruchart, and M. G. Lorthioir, *J. Phys. (Paris) Colloq. (Pt. 2)* **C1**, 982–984 (1971).
12. R. Juza, W. Gieren, and J. Haug, *Z. Anorg. Allg. Chem.* **300**, 61–71 (1959); R. Juza and J. Haug, *Z. Anorg. Allg. Chem.* **309**, 276–282 (1961).
13. A. P. Palisaar and R. Juza, *Z. Anorg. Allg. Chem.* **384**, 1–11 (1971);

- D. Halot and J. Flahaut, *C. R. Acad. Sci. Ser. C* **272**, 465–467 (1971).
14. P. Höhn, R. Kniep, and J. Maier, *Z. Naturforsch. B* **49**, 5–8 (1994).
15. A. Gudat, R. Kniep, and J. Maier, *J. Alloys Compd.* **186**, 339–345 (1992), and references therein.
16. P. Höhn and R. Kniep, *Z. Naturforsch. B* **47**, 434–436 (1992).
17. P. Höhn, S. Haag, W. Milius, and R. Kniep, *Angew. Chem. Int. Ed. Engl.* **30**, 831–832 (1991).
18. X. Z. Chen, D. L. Ward, and H. A. Eick, *J. Alloys Compd.* **206**, 129–132 (1994).
19. D. A. Vennos and F. J. DiSalvo, *Acta Crystallogr.* **48**, 610–612 (1992).
20. Ch. Wachsmann and H. Jacobs, *J. Alloys Compd.* **190**, 113–116 (1992).
21. F. K.-J. Helmlinger, P. Höhn, and R. Kniep, *Z. Naturforsch. B* **48**, 1015–1018 (1993).
22. We have prepared this compound but not reported its structure.
23. G. M. Sheldrick, in "Crystallographic Computing 3" (G. M. Sheldrick, C. C. Kruger, R. Doddard, Eds.), pp. 175–189. Oxford Univ. Press, Oxford, 1985.
24. Function minimized: $\sum w(F_o^2 - F_c^2)^2$, where $w = 4F_o^2/\sigma^2(F_o^2)$.
25. D. T. Cromer and J. T. Waber, "International Tables for X-ray Crystallography," Vol. IV. Table 2.2 A. Kynoch Press, Birmingham, 1974.
26. "TEXSAN-TEXRAY Structure Analysis Package," Molecular Structure Corporation, The Woodlands, TX, 1985.
27. S. C. Lee, J. Li, J. C. Mitchell, and T. H. Holm, *Inorg. Chem.* **31**, 4333–4338 (1992).
28. R. X. Fischer and E. Tillmanns, *Acta Crystallogr. Sect. C* **44**, 775–776 (1988).